Selection of automotive brake friction composites reinforced by agro-waste and natural fiber: An integrated multi-criteria decision-making approach

Tej Singh [a,*], Gustavo da Silva Gehlen [b,1], Vedant Singh [c], Ney Francisco Ferreira [b,1], Liu Yesukai de Barros [b,1], Germano Lasch [b,1], Jean Carlos Poletto [b,1], Sharafat Ali [d], Patric Daniel Neis [b,1]

[a] Savaria Institute of Technology, Faculty of Informatics, ELTE Eötvös Loránd University, Budapest, 1117, Hungary
[b] Laboratory of Tribology, Federal University of Rio Grande do Sul, Osvaldo Aranha 99, Porto Alegre, Brazil
[c] Amrita School of Business, Amrita Vishwa Vidyapeetham, Bengaluru, 560035, India
[d] Allied Nippon Private Limited, Sahibabad, UP, 201010, India

ARTICLE INFO

ABSTRACT

The aim of this study is to develop a method for selecting and ranking automotive brake friction composite materials made from agro-waste and natural fibers. This is achieved by using an integrated multi-criteria decision-making methodology. Consequently, six composite samples are produced by reinforcing rice husk, rice husk ash, and *Grewia optiva* fiber. These samples are then assessed for their frictional properties using a laboratory-scale brake tribometer, in accordance with the requirements outlined in SAE J2522 standard. The selection criteria are based on the analyzed tribological parameters, which include friction coefficients, wear, and friction fluctuations fade-recovery performances. The CRITIC (criteria importance through intercriteria correlation) method was used to determine the importance of criteria for performance evaluation. Based on CRITIC analysis, the average friction coefficient (0.1592), recovery-3 (0.1363), friction fluctuations (0.1347), and performance friction coefficient (0.1240) were identified as the key criteria. The use of MARCOS (measurement of alternatives and ranking according to compromise solution) for ranking assessment reveals that composite materials reinforced with rice husk ash exhibit the most favorable tribological characteristics. The validation of the ranking using different decision-making tools demonstrates the reliability and effectiveness of the proposed approach.

1. Introduction

The use of lignocellulosic materials, such as agro-wastes and natural fibers, in the design of brake friction composite materials offers several benefits, including a reduction in reliance on conventional materials and environmental protection [1,2]. However, attaining the appropriate tribological characteristics in a brake friction composite application is a complex task that requires focused endeavors to fulfill the rigorous performance standards established by several regulatory entities [3,4]. These criteria encompass attributes like stable friction, minimal wear, rapid recovery, and limited fade under diverse operating conditions, including vehicle speed, braking force, duration, and temperature variations [5,6]. To achieve these desired performance characteristics, brake friction materials consist of a carefully balanced combination of 10–20 ingredients. These components can be broadly categorized into

four classes: fibers, fillers, binders, and friction modifiers [7]. Fiber is a very significant component due to its ability to enhance strength, optimize the tribological characteristics of friction materials, and address the limitations arising from the improper selection of components, hence alleviating intrinsic compositional defects [8–10]. Typically, friction materials use ceramic, metallic, and organic fibers either individually or in various combinations [7–10]. Currently, the conventional reinforcing materials commonly utilized, including, Kevlar fibers, carbon fibers, and glass fibers, exhibit several drawbacks. These drawbacks encompass their non-biodegradability, limited recycling capabilities, potential health hazards when inhaled, high density, substantial energy consumption during manufacturing, and elevated production costs [11, 12]. In recent years, there has been a significant focus on life cycle analysis, particularly in relation to composites made from lignocellulosic materials [13,14]. These composites have garnered considerable

---

attention and recognition due to their ability to decrease carbon dioxide emissions over their entire life cycle, in contrast to composites made from synthetic fibers [15]. Furthermore, the manifold advantageous attributes of lignocellulosic materials, including their low density, biodegradability, renewability, cheap or negligible cost, widespread availability, non-toxic and non-abrasive nature, contribute to their high demand in diverse applications [16–18].

In recent years, several research endeavors have been undertaken to explore the potential of using lignocellulosic materials, including agro-wastes and natural fibers, in the production of friction composite materials. Akıncıoğlu et al. [19] compared the sliding wear and friction characteristics of a brake friction composite filled with hazelnut shell waste to a commercially available composite material in their study. The study discovered that the friction characteristics of hazelnut shell waste (7 wt%) reinforced composites outperform commercial samples. This enhancement, however, comes at the expense of increased wear. Akıncıoğlu et al. [20] conducted a study to investigate the effects of adding walnut shell waste at concentrations of 3.5 wt% and 7 wt% on the tribological properties of brake friction composites. The investigation was carried out following the SAE-J661 test standards. The researchers determined that composites containing a lower percentage of walnut shell waste (3.5 wt%) demonstrate a higher degree of resistance to wear. Conversely, it was demonstrated that composites with a higher proportion (7 wt%) of walnut shell waste displayed an elevated friction coefficient. Chandradass et al. [21] conducted a study on the development of a new type of brake pad materials for automobiles. More precisely, they incorporated sugarcane bagasse ash into the brake pad composition at concentrations of 5 wt% and 10 wt%. The main aim of their investigation was to evaluate the sliding wear and friction properties of these recently manufactured materials. According to the authors' findings, there was a direct correlation between the increase in bagasse ash loading and the increase in wear of the brake pads. Furthermore, it was noted that brake pads containing 5 wt% of bagasse ash demonstrated improved friction performance in comparison to other loadings. The effectiveness of fly ash and bagasse ash (0–12% by weight) on the performance of phenolic-based automotive brake friction composites was examined by Choosri et al. [22]. The authors stated that in phenolic-based brake friction composites, bagasse ash and fly ash have demonstrated great promise as substitute abrasives for silica and alumina. According to the findings, it was advised to add 4 wt% of fly ash and bagasse ash to optimize the brake friction composites' overall characteristics.

Among the agro-wastes, rice husk and its ash have been found to be effective in improving the mechanical, tribological, and thermal properties of polymer composites due to their high silica content [23–26]. The raw rice husk was found to have a silica content of 15–20%, whereas rice husk ash was found to contain over 90% silica content [27,28]. Silica is classified as an abrasive and is commonly used as one of the main ingredients in various commercial brake friction material formulations. Literature reports the utilization of rice husk and its ash in the fabrication of automotive brake friction materials. Mutlu [29] conducted a study to examine the relative effectiveness of rice straw and rice husk (at 4% and 20% weight ratios) in real-world brake friction materials. The study determined that the brake material containing 20 wt% rice husk exhibited superior friction characteristics, albeit at the expense of increased wear. Mutlu and Keskin [30] conducted a study to examine how the addition of rice straw powder (ranging from 5% to 25% of the total weight) affects the wear and friction characteristics of friction composites. The study found that the inclusion of 15 wt% rice straw powder in composites led to improved wear and thermo-mechanical properties compared to other combinations. The effect of rice husk loadings (from 0% to 12% by weight) on the tribological performance of brake friction materials was studied by Gehlen et al. [31]. The composites' wear resistance decreased with increasing rice husk loadings at lower temperatures (300 °C), while at higher temperatures (550 °C), the fade resistance decreased, and the friction

instability increased. The formulation containing 6 wt% rice husk content was determined to be superior to the others, exhibiting the least amount of wear. Nogueira et al. [32] conducted a study to examine the impact of rice husk (grinded and heat treated) on the tribological properties of phenolic composites. They compared these properties with a formulation that substituted alumina for rice husk. Friction materials that incorporate rice husk (grinded and heat treated) have demonstrated promising characteristics, including a friction coefficient and wear rate that are comparable to those of alumina-based formulations. In general, the use of rice husk and its ash in brake composite formulations has been shown to enhance the stability of friction performance by creating secondary contact plateaus [33,34].

In recent years, researchers have examined natural fibers as potential environmentally-friendly reinforcing elements for automotive brake friction materials. Ramie, hemp, kenaf, pineapple, *Areva javanica* and banana are just some of the plants that have been tried and tested [35–37]. The friction and wear performance exhibited by natural fiber reinforced composites is demonstrated to be satisfactory, often approaching that of standard commercial friction materials, thereby indicating their comparable braking power. Rajan et al. [38] assessed phenolic composites filled with slag waste and reinforced with coir fiber (5%–20% by weight). The researchers documented that incorporating a lower amount of coir fiber (5 wt%) resulted in favorable outcomes in terms of friction, fade, and wear. In contrast, composites containing a greater weight percent (20 wt%) of coir fiber demonstrated exceptional recovery characteristics, albeit at the expense of reduced friction performance. The impact of corn stalks fiber (ranging from 4% to 12% by weight) on the fade-recovery capabilities of brake composites reinforced with glass fiber were investigated by Liu et al. [8]. According to the authors, the composite containing 6 wt% corn stalk fiber has the greatest recovery ratio and the lowest fade ratio, whereas the composite containing 10 wt% corn stalk fiber demonstrated a comparatively low fade/recovery fluctuation. Composites containing the smallest proportion of corn stalk fiber (4 wt%) demonstrated the most unfavorable friction behavior in the fade test. The research suggested that composites containing 10 wt% corn stalk fibers demonstrated exceptional recovery and resistance to fading, as well as a high degree of frictional stability throughout the fade and recovery tests. Furthermore, numerous studies have been conducted on the impact of brake friction materials that include a natural fiber content of up to 20 wt%. In these studies the composites containing a lower proportion of natural fibers (≤10 wt%) have been found to demonstrate higher coefficients of friction, better fade performance, greater friction stability, and improved wear resistance, with minimal fluctuations in friction. Conversely, composites containing a higher proportion of natural fibers (≥15 wt%) demonstrate superior recovery performance, albeit at the expense of reduced friction and fade performance [37–39].

The existing research places a growing emphasis on the fact that the choice of lignocellulosic materials and their respective ratios typically have an impact on the tribological characteristics (such as coefficient of friction, wear, fade, and recovery) of the composite material. Given that each produced composite has a unique performance characteristic, it is necessary to determine the optimal composite that exhibits the maximum degree of satisfaction across all material attributes [40]. One way to do this is by use multi criteria decision making (MCDM) techniques. MCDM techniques are systematic approaches that use logical ways to assess the significance of criteria (i.e., material attributes) in relation to a specific application [41,42]. These techniques aid in selecting the most acceptable material candidate and eliminating inappropriate alternatives. Several MCDM techniques have been created to assist in the evaluation and selection of the most suitable alternative materials. These approaches include TOPSIS, MARCOS, COPRAS, GRA, PROMETHEE, MOORA, ELECTRE, CoCoSo, and ARAS, among others [40–47]. The MARCOS methodology stands out as an effective ranking method due to its straightforward mathematical computations and user-friendly nature, in comparison to other MCDM techniques [48].

Conversely, specific MCDM problems utilize the CRITIC method to determine the weights of criteria (material property importance) [49]. Ranking alternatives is thus possible through the utilization of these two approaches. Hence, automotive brake friction materials reinforced with rice husk and *Grewia optiva* fiber, which were previously manufactured and evaluated for their tribological properties, were utilized in the current investigation [34,39]. Owing to the challenges associated with choosing the best-manufactured automotive brake friction composites, a hybrid approach known as CRITIC-MARCOS has been suggested. The evaluated tribological characteristics are set as the selection criteria, the criterion weight is determined using CRITIC and the final composite ranking is obtained using the MARCOS technique.

2. Experimental procedure

2.1. Materials and composite fabrication

A total of twelve ingredients were chosen for the production of the friction composite. These include phenolic resin as a binder, lapinus fiber, steel fiber, ceramic, and *Grewia optiva* fiber as the reinforcement, calcium carbonate and barite as space fillers, alumina and graphite as property modifiers, and vermiculite, rice husk, and rice husk ash as functional fillers. The *Grewia optiva* fiber used in this study originates from the Dehlwin village situated in the Bilaspur area of Himachal Pradesh, India. The natural fiber was hand trimmed to fiber lengths ranging from 2 to 6 mm. The rice husk was gathered from the southern area of Brazil. The rice husk was further pulverized to achieve a particle size of ≤350 μm. To acquire the ash, the rice husk underwent a heating process at a temperature of 600 °C for duration of 2 h in an oven equipped with air circulation. This procedure was carried out to eliminate all the organic compounds present. The outcome of this procedure was rice husk ash, rich in silica content characterized by its white powdery form.

Table 1 lists the several friction formulations and their component amounts along with their nomenclature and composition data. It is worth noting that there are two main groups of formulations, each sharing the same basic materials. The group I comprises formulations A1 to A4, where the amount (in wt.%) of ceramic and *Grewia optiva* is changed. The group II comprises formulations A5 and A6, where the type of natural abrasive (rice husk or rice husk ash) is changed. The ingredients of the formulations of group I were mixed using a high rotation shear mixer (Fabdecon Engineers, India) with a chopper speed of 3000 rev/min. To reach a uniform dispersion, the fibrous elements were blended with phenolic resin for 5 min, and then the powdered materials were added and mixed for a further 5 min. Next, 80 g of the resulting mixture was put into an iron mold. The prepared mold was heated for 8 min at 155 °C under 150 bar of pressure in a compression molding machine made by Fabdecon Engineers, India. To get rid of the volatiles created during the cure process; compression molding was

done with four sporadic breathing cycles. After being taken out of the mold, the cured composites were allowed to cool at ambient temperature before being post-cured in an oven at 160 °C for 3h. For the formulations of group II, rice husk was thermally treated for 2 h at 110 °C before being added to the mixture, to ensure the release of all moisture. After that, all the ingredients of each formulation were blended for 30 min using a WAB T2F Turbula mixer. By utilizing a Buehler Pneumet I mounting press, cylindrical pins measuring 14 mm in diameter and 15 mm in height were created. A pressure of 100 MPa was applied during the 10-min hot molding operation at 150 °C. The pins were then subjected to a post-curing procedure in a muffle furnace for 4 h at 200 °C, which is close to the cycle used for genuine brake pads. The fabrication methodology is described in full elsewhere [34,39]. Subsequently, all the post-cured composites were subjected to machining, resulting in specimens with a cylindrical shape, each cylinder with a diameter of 14 mm and a height of 7 mm. These specimens were then securely attached to a backplate (Fig. 1a), enabling their use in tribological testing. Fig. 2b displays a scanning electron microscope (SEM) picture of the fabricated composite, indicating the existence of several primary components.

2.2. Tribological characterization

The experiments were carried out in an LSBT (laboratory-scale braking tribometer). This apparatus replicates the working conditions (temperature, velocity, and contact pressure) encountered in actual vehicle braking systems [50]. The LSBT controls the starting temperature of each braking operation through an induction heating system, as can be seen on Fig. 2. This apparatus continually measures the temperature using a K-type thermocouple embedded in the brake disc and calculates the coefficient of friction (COF) throughout the entire testing procedure [51].

The tribological characterization followed the requirements of the SAE J2522 (AK Master) standard for brake pads. The brake industry uses this methodology all around the world since it can assess the performance of a brake material in a variety of circumstances. The sections of the procedure are listed in Table 2 [52]. The AK Master test was carried out for three samples of each formulation (A1 to A6), in a total of eighteen tests. A comprehensive examination of the wear mechanisms and surface structures of the friction composites was achieved by analyzing images of the samples' worn surfaces. The scanning electron microscope (SEM, TM3000 Tabletop Microscope-Hitachi) was utilized to obtain those images.

2.3. CRITIC-MARCOS optimization

2.3.1. CRITIC method

The CRITIC method employs criteria dispersion and conflict intensity as considerations for weighting. The degree of dispersion quantifies the extent to which evaluation criteria may vary significantly. The degree of conflict is indicative of the degree of similarity between the various criteria. A higher degree of dispersion and disagreement amongst criteria calls for a greater weight. The steps below are used to carry out the CRITIC method [49,53].

Step 1 The first step in decision-making is to construct a matrix. A decision matrix is created by defining a collection of p alternatives and q criteria, which are included in multi-criteria models as follows.

$$[Z_{ij}]_{p \times q} = \begin{array}{c} \\ A_1 \\ A_2 \\ \vdots \\ A_i \\ \vdots \\ A_p \end{array} \overset{\begin{array}{cccccc} c_1 & C_2 \nearrow \cdots & C_j \nearrow \cdots & C_q \end{array}}{\begin{bmatrix} Z_{11} & Z_{12} & \cdots & Z_{1j} & \cdots & Z_{1q} \\ Z_{21} & Z_{22} & \cdots & Z_{2j} & \cdots & Z_{2q} \\ \vdots & \vdots & \cdots & \vdots & \cdots & \vdots \\ Z_{i1} & Z_{i2} & \cdots & Z_{ij} & \cdots & Z_{iq} \\ \vdots & \vdots & \cdots & \vdots & \cdots & \vdots \\ Z_{p1} & Z_{p2} & \cdots & Z_{pj} & \cdots & Z_{pq} \end{bmatrix}} \quad (1)$$

Table 1
Nomenclature and compositional detail.

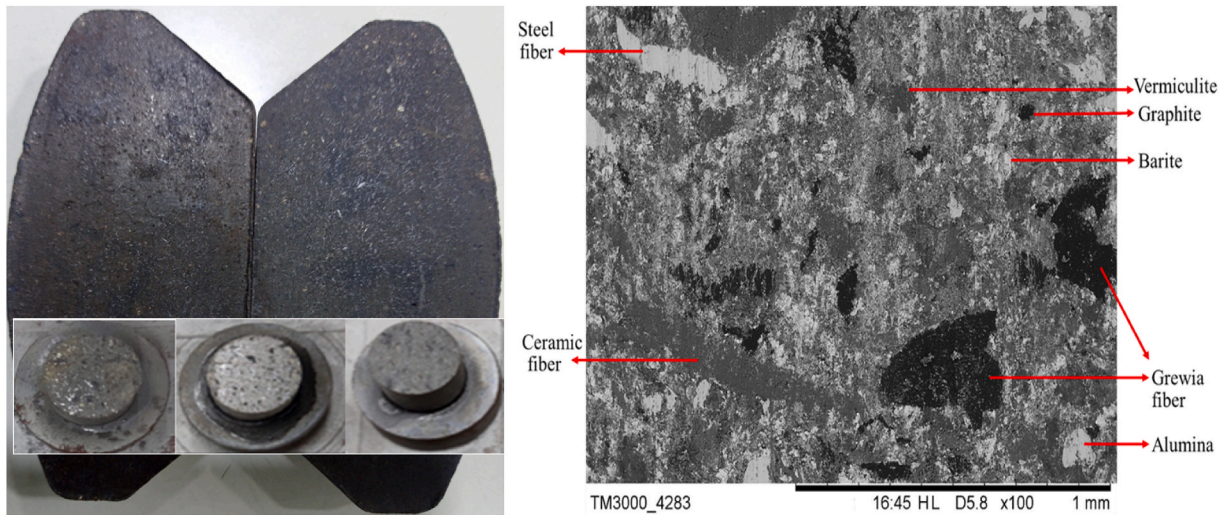| Materials (wt.%)	Nomenclature/Alternatives					
	A1	A2	A3	A4	A5	A6
Phenolic resin	10	10	10	10	12	12
Barite	50	50	50	50	30	30
Calcium carbonate	0	0	0	0	23	23
Graphite	6	6	6	6	8	8
Alumina	3	3	3	3	6	6
Vermiculite	5	5	5	5	0	0
Steel fiber	6	6	6	6	15	15
Lapinus fiber	10	10	10	10	0	0
Ceramic fiber	7.5	5	2.5	0	0	0
Grewia optiva fiber	2.5	5	7.5	10	0	0
Rice husk	0	0	0	0	6	0
Rice husk ash	0	0	0	0	0	6

Fig. 1. (a) Composite samples (14 mm in diameter), and (b) Microscopic image of the untested composite surface.
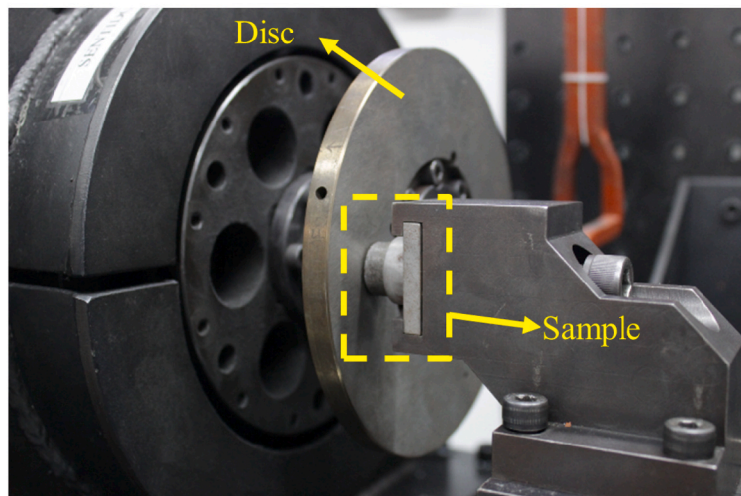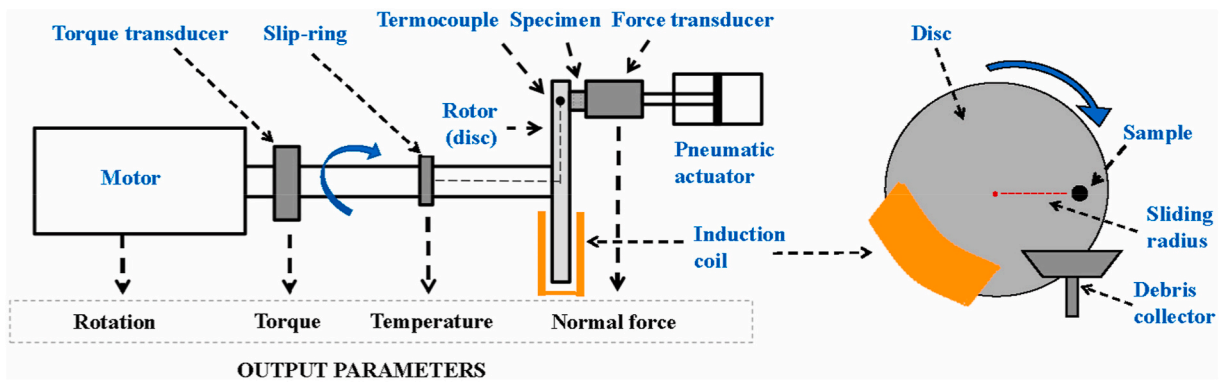

Fig. 2. Laboratory-scale braking tribometer used to carry out the automotive braking tests: (a) schematic representation and (b) image of the contact between the disc and the sample.

Where Z_{ij} signifies the value of i-th alternative for j-th criterion.

Step 2 Decision-matrix is normalization. The structured decision-matrix is normalized for the beneficial (N_b) and non-beneficial (N_{nb}) criteria:

$$r_{ij} = \frac{Z_{ij} - \min(Z_{ij})}{\max(Z_{ij}) - \min(Z_{ij})} \nearrow if\ j \in N_b \tag{2}$$

$$r_{ij} = \frac{\max(Z_{ij}) - Z_{ij}}{\max(Z_{ij}) - \min(Z_{ij})} \nearrow if\ j \in N_{nb} \tag{3}$$

Step 3 The standard deviation (S_j) of each criterion determined to measure the dispersion degree using following equation:

Table 2
SAE J2522 test procedure.

Section	Description
1. Green characteristic	Applications = 30, pressure = 30 bar, Initial brake temperature (IBT) = 100 °C, speed = 80-30 km/h
2. Burnish	Applications = 64, pressure = 15–51 bar, IBT = 100 °C, speed = 80-30 km/h
3. Characteristic value	Applications = 6, pressure = 30 bar, IBT = 100 °C, speed = 80-30 km/h
4.Speed/pressure sensitivity (SPS)	Applications = 8, pressure = 10–80 bar, IBT = 100 °C, speed = 40-5 km/h
	Applications = 8, pressure = 10–80 bar, IBT = 100 °C, speed = 80-40 km/h
	Applications = 8, pressure = 10–80 bar, IBT = 100 °C, speed = 120-80 km/h
	Applications = 8, pressure = 10–80 bar, IBT = 100 °C, speed = 160-130 km/h
	Applications = 8, pressure = 10–80 bar, IBT = 100 °C, speed = 200-170 km/h
5. Characteristic value	Applications = 6, pressure = 30 bar, IBT = 100 °C, speed = 80-30 km/h
6. Cold	Applications = 1pressure = 30 bar, IBT = 40 °C, speed = 40-5 km/h
7. Characteristic value	Applications = 18, pressure = 30 bar, IBT = 100 °C, speed = 80-30 km/h
8. Fade 1	Applications = 15, deceleration = 0.4 g, IBT = 100–550 °C, speed = 100-5 km/h
9. Recovery 1	Applications = 18, pressure = 30 bar, IBT = 100 °C, speed = 80-30 km/h
10. Temperature/pressure sensitivity (TPS)	Applications = 8, pressure = 10–80 bar, IBT = 100 °C, speed = 80-30 km/h
	Applications = 9, pressure = 30 bar, IBT = 100–500 °C, speed = 80-30 km/h
	Applications = 8, pressure = 10–80 bar, IBT = 500 °C, speed = 80-30 km/h
11. Recovery 2	Applications = 18, pressure = 30 bar, IBT = 100 °C, speed = 80-30 km/h
12. Fade 2	Applications = 15, deceleration = 0.4 g, IBT = 100–550 °C, speed = 100-5 km/h
13. Recovery 3	Applications = 18, pressure = 30 bar, IBT = 100 °C, speed = 80-30 km/h

$$\begin{cases} S_j = \sqrt{\dfrac{\sum_{i=1}^{p}\left(r_{ij} - \overline{r}_j\right)^2}{p-1}} \\ \overline{r}_j = \dfrac{\sum_{i=1}^{p} r_{ij}}{p} \end{cases} \tag{4}$$

Step 4 Calculation of conflict degree between criterion using following equation.

$$\Re_j = \sum_{\substack{i=1 \\ i \neq j}}^{q} \left(1 - \nu_{ij}\right) \tag{5}$$

Where ν_{ij} represent the correlation coefficient between i-th and j-th criteria.

Step 5 Weight calculation

The formula for j-th criterion weight calculation is given as:

$$\omega_j = \frac{\Re_j \times S_j}{\sum_{j=1}^{q} \Re_j \times S_j} \tag{6}$$

2.3.2. MARCOS method

The MARCOS MCDM tool was presented by Stević et al. [48] for the purpose of healthcare supplier prioritization. The MARCOS model is used to tackle a variety of decision-making challenges because of its easy

calculation [54–56]. The following are the steps of the MARCOS method [54–56].

Step 1 Formation decision-making matrix. The initial decision matrix ($[Z_{ij}]_{p \times q}$) is extended by adding the ideal value (IV) and anti-ideal value (AIV) and given as.

$$[Z_{ij}]_{p \times q} = \begin{array}{c} \\ A_{AIV} \\ A_1 \\ A_2 \\ \vdots \\ A_i \\ \vdots \\ A_p \\ A_{IV} \end{array} \overset{\begin{array}{cccccc} c_1 & C_2 & \cdots & C_j & \cdots & C_q \end{array}}{\begin{bmatrix} Z_{AIV1} & Z_{AIV1} & \cdots & Z_{AIVj} & \cdots & Z_{AIVq} \\ Z_{11} & Z_{12} & \cdots & Z_{1j} & \cdots & Z_{1q} \\ Z_{21} & Z_{22} & \cdots & Z_{2j} & \cdots & Z_{2q} \\ \vdots & \vdots & \cdots & \vdots & \cdots & \vdots \\ Z_{i1} & Z_{i2} & \cdots & Z_{ij} & \cdots & Z_{iq} \\ \vdots & \vdots & \cdots & \vdots & \cdots & \vdots \\ Z_{p1} & Z_{p2} & \cdots & Z_{pj} & \cdots & Z_{pq} \\ Z_{IV1} & Z_{IV2} & \cdots & Z_{IVj} & \cdots & Z_{IVq} \end{bmatrix}} \tag{7}$$

The IV and AIV are determined based on the following equations.

$$IV = \max\left(Z_{ij}\right) \, if\ j \in N_b, and\ IV = \min\left(Z_{ij}\right) \, if\ j \in N_{nb} \tag{8}$$

$$AIV = \max\left(Z_{ij}\right) \, if\ j \in N_{nb}, and\ AIV = \min\left(Z_{ij}\right) \, if\ j \in N_b \tag{9}$$

Step 2 The updated decision matrix normalized in the range of 0–1 using following equations.

$$z_{ij} = \frac{Z_{ij}}{Z_{IV}} \, if\ j \in N_b \tag{10}$$

$$z_{ij} = \frac{Z_{IV}}{Z_{ij}} \, if\ j \in N_{nb} \tag{11}$$

Step 3 Weighted normalized decision matrix is constructed using following equation.

$$\varpi_{ij} = \omega_j \times z_{ij} \tag{12}$$

Step 4 Calculation of sum of the weighted matrix values using following equation.

$$k_i = \sum_{i=1}^{p} \varpi_{ij} \tag{13}$$

Step 5 Calculation of the utility degree of alternatives. In relation to IV and AIV, the utility degrees are determined using following equations.

$$k_i^+ = \frac{k_i}{k_{IV}}, and\ k_i^- = \frac{k_i}{k_{AIV}} \tag{14}$$

Step 6 Concerning the IV and AIV the utility functions are calculated using following equations.

$$f\left(k_i^+\right) = \frac{k_i^-}{k_i^+ + k_i^-}, and\ f\left(k_i^-\right) = \frac{k_i^+}{k_i^+ + k_i^-} \tag{15}$$

Step 7 The determination of final utility function of alternatives using following formula.

$$f(k_i) = \frac{k_i^+ + k_i^-}{1 + \frac{1 - f\left(k_i^+\right)}{f\left(k_i^+\right)} + \frac{1 - f\left(k_i^-\right)}{f\left(k_i^-\right)}} \tag{16}$$

Step 8 Ranking the alternatives. The alternatives are ranked from best to worst by descending order of their $f(k_i)$ values.

3. Results and discussion

3.1. Tribological results of the composites

3.1.1. μ_P and wear results

The coefficient of friction (COF) results of the composites by the application of 274 braking in total for different sections (listed in Table 2) are shown in Fig. 3. Significant fluctuations in COF are evident throughout the SPS braking section (braking instance #101 to #140), as well as from braking instance #173 to the conclusion of the test (braking instance #274). Braking instance #173 to #274 belongs to sections that are specifically connected to the high temperature sensitivity section.

Regarding the influence of various testing circumstances on the coefficient of friction (COF), numerous performance metrics are considered, including performance COF (μ_P), specific wear rate (SWR), average COF (μ_avg), friction fluctuations (Δμ), %-fade resistance (%-FR) and %-recovery (%-R). The data was gathered from many test sections, as shown in Table 1, which were previously used in prior research. The μ_P was determined by taking the average of the recorded values for the braking applications for the characteristic value (section 3, 5 and 7) and recovery (section 9, 11 and 13) test sections of the SAE J2522 test protocol. The weight loss of the composite samples was assessed after the test cycle in order to calculate the SWR. The SWR of the composites was calculated using following formula [39].

$$SWR = \frac{\Delta \omega}{\rho \times D \times F} \qquad (17)$$

Here, $\Delta \omega$ = composite sample weight loss (g), F = friction force (N), D = sliding distance (m), and ρ = composite sample density (g/cm^3).

The μ_P (the higher, the better) and SWR (the lower, the better) results of the investigated composite alternatives are presented in Fig. 4. Overall, based on results from Fig. 4, it is seen that either a combination of *Grewia optiva* with ceramics (samples A1 to A3) or the sample with only *Grewia optiva* (A4) are good for the μ_P. In particular, the combination of 5 wt% of *Grewia optiva* fiber with 5 wt% of ceramic fiber (sample A2) presented the best μ_P (0.44) among all composite alternatives. On the other hand, sample with rice husk (sample A5) showed the poorest μ_P with a value of 0.35. This can partially be attributed to the fact that rice husk is the sample with the lowest amount of hard abrasive fibers (only 6 wt% of alumina). The sample with rice husk ash (sample A6) also exhibited a good μ_P (0.43), since ash contain substantial amount of silica which is a hard abrasive along with 6 wt% alumina and 15 wt% steel fiber. It is worth noting that A5 and A6 have a different basic composition. In this case, the natural fiber (rice husk – A5; or rice husk ash – A6) seems to be the main contributor for the poor and good μ_P (A5
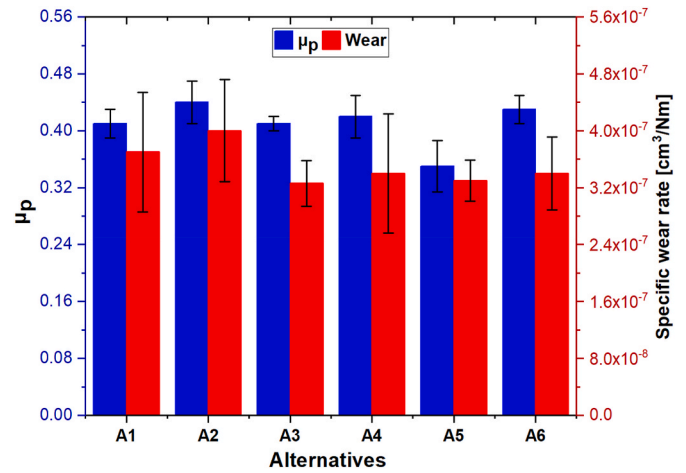

Fig. 4. μ_p and SWR results of the evaluated composites.

and A6, respectively), since between those samples (A5 and A6) only the type of fiber (rice husk and rice husk ash) is changed. In case of the *Grewia optiva* fiber contained samples, their formulations have a combination of different types of hard abrasive fibers, i.e. ceramics (0.0–7.5 wt%), alumina (3 wt%) and also rock fibers (lapinus fiber, 10 wt%). Regarding the SWR presented in Fig. 4, it can be seen that the A1/A2 formulations exhibited higher wear (3.85 ± 0.15 × 10^{-7} cm^3/Nm), while the magnitudes of wear remain very close (3.33 ± 0.07 × 10^{-7} cm^3/Nm) in formulations A3 to A6. The composite samples A3 (3.26 × 10^{-7} cm^3/Nm) and A2 (4 × 10^{-7} cm^3/Nm) showed the best and the worst wear performance, respectively. Wear was observed to diminish continuously as the organic content increased, as evidenced by the incorporation of Grewia optiva fiber in formulations A3/A4 and rice husk, rice husk ash, graphite, and phenolic resin in formulations A5/A6. The shear thinning rheology of an increasing organic content rich friction film at composite surfaces results in wear mitigation and stability, as found experimentally. Different studies have shown similar findings on wear minimization using organic ingredients [37,57]. The result shows that a right balance between the content of natural fiber (*Grewia optiva*) and ceramic is important to reach a good SWR. Another interesting result is the fact that the composite alternatives with rice husk (i. e. A5) and rice husk ash (i.e. A6) did not differ that much from the sample with the best SWR (A3). This means that the wear performance of the samples with rice husk and rice husk ash can also be considered relatively satisfactory.
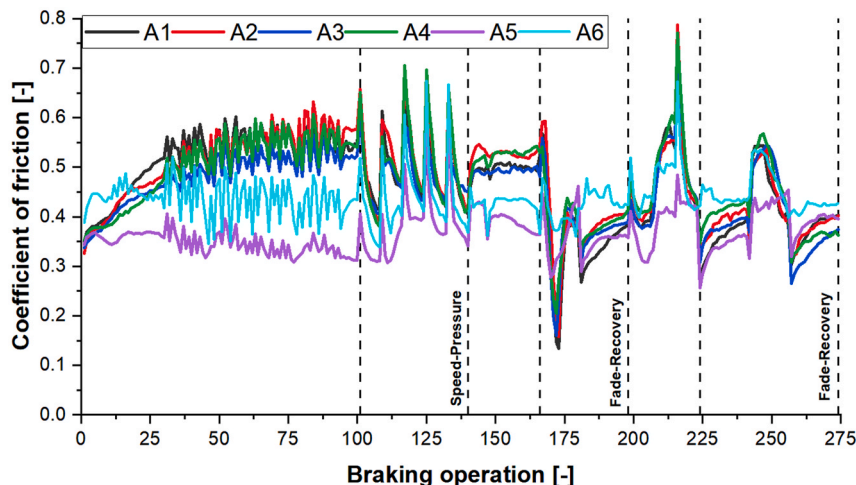

Fig. 3. Mean COF per braking application for the entire test procedure.

3.1.2. Sensitivity of COF towards speed-pressure

The speed-pressure sensitivity (SPS) of a brake friction material is a crucial factor in determining its stability when subjected to different pressure/speed conditions. For optimal braking performance, it is advised to choose a friction material with a high COF that exhibits minimal changes in the presence of speed and pressure variations. There are 40 braking instances for SPS section (#101-#140), eight for each brake-release speed at 10–80 bar pressure, as described in Table 1. The μ_{avg} was the average of COF collected during SPS test section from the braking instance #101 to #140. Whereas the $\Delta\mu$ is the difference between the maximum and minimum COF recorded for the for SPS section (#101-#140). The variations of μ_{avg} (the higher, the better) and $\Delta\mu$ (the lower, the better) of the investigated alternatives are depicted in Fig. 5. From Fig. 5 it is observed that the alternative A2 exhibits highest μ_{avg} (0.510) whereas alternative A5 shows the lowest μ_{avg} of 0.390.

However, the composites with *Grewia optiva* content (A1-A4) exhibited higher μ_{avg} (0.496 $\pm$ 0.014) as compared to the rice husk and rice husk ash loaded composites (i.e. A5/A6) with a μ_{avg} value of 0.419 $\pm$ 0.029. This variation in μ_{avg} for *Grewia optiva* based composite is mainly ascribed to the presence of ceramic and lapinus fiber, which are not present in group II (A5/A6). Regarding friction stability, which is measured in terms of $\Delta\mu$ in the SPS cycle, the alternative A3 shows the lowest $\Delta\mu$ (0.197) whereas alternative A5 shows the highest $\Delta\mu$ value of 0.337. The composite A3 (2.5/7.5 wt% of ceramic and *Grewia optiva*, respectively) exhibited the best result among all samples. This is in good agreement with [57], where the researchers also tested formulations with organic and ceramic fibers combined. The authors of the study also discovered that composites with a high concentration of organic fiber ($\geq$7.5 wt%) and a lower quantity of ceramic fiber exhibited excellent friction stability, characterized by a low $\Delta\mu$.

3.1.3. Sensitivity of COF towards temperature

The sensitivity of COF to temperature is analyzed in terms of fade-recovery characteristics, which are one of the most important aspects for rating the performance of any brake friction material. The purpose of the fade section is to evaluate the decrease in COF performance under high temperature conditions, while the recovery section is used to examine its restoration to normal performance. There are two fade sections (section 8, and 12) each of 15 brakes and three recovery sections (section 9, 11 and 13) each of 18 brakes are mentioned in SAE J2522 test procedure. The recorded COF during these sections was assessed in terms of %-fade resistance (%-FR) and %-recovery (%-R) using following equations [39]:

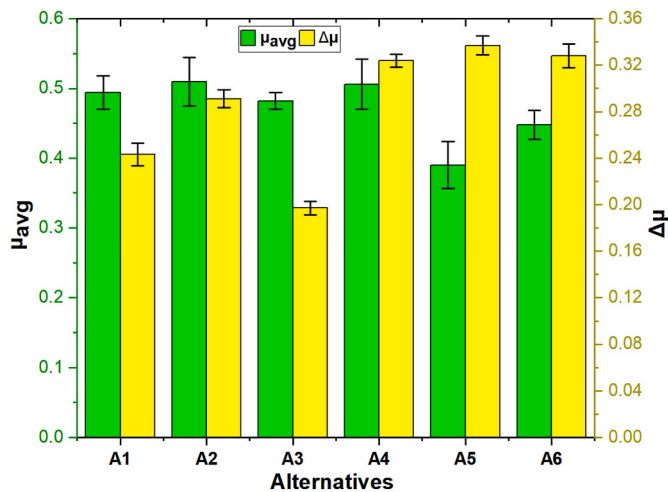$$\% - FR = \frac{\mu_f}{\mu_P} \times 100 \qquad (18)$$

$$\% - R = \frac{\mu_r}{\mu_P} \times 100 \qquad (19)$$

Here, μ_P = performance COF, μ_r = average COF for the respective recovery (recovery 1/recovery 2/recovery 3) section, and μ_f = lowest COF for the respective fade (fade 1/fade 2) section.

The results of %-FR (the higher, the better) and %-R (the higher, the better) for the investigated composite alternatives are depicted in Figs. 6 and 7, respectively. As evident from Fig. 6, the lowest %-FR1 was noted for composite alternative A1 having 2.5 wt% *Grewia optiva* fiber content and remained highest in the alternative A6 with 6 wt% of rice husk ash content. The analyzed composite alternatives exhibited a very narrow range of fluctuation in their %-FR2, with values ranging from 86.93% $\pm$ 5.87%. About the fade resistance (Fig. 6), it is clear the superior performance of the sample A6 with rice husk ash content, since it presented the best %-FR in both fade 1 (%-FR1 = 84.2%) and fade 2 (%-FR2 = 92.8%). Three main reasons may explain this behavior: (1) sample A6 formed large area fraction of contact plateaus in the fades 1 and 2, which acted to prevent the deterioration of the sample's ingredients. More details can be found in Ref. [34]; (2) sample A6 contains 6 wt% of rice husk ashes, which are basically silica. This compound (silica) presents good resistance at high temperatures; (3) it is also necessary to consider that the basic materials of A5 and A6 are slightly different from A1 to A4. This may also influence the fade performance. Another interesting behavior observed for all samples (A1 to A6, i.e. *Grewia optiva*, rice husk and rice husk ash) is a poorer performance in fade 1 compared to fade 2. This is because the fade 1 is the first time where the friction materials underwent high temperatures (>350 °C) during the Ak-Master test procedure. This behavior (the poorer performance in fade 1) is consistent with previous papers [31]. Possible explanations for a lower %-FR1 are the higher degradation in the phenolic resin and natural ingredients (*Grewia optiva* and rice husk) of the composites [58] during the first time the friction material is subjected to elevated temperatures, as well as some irreversible chemical processes under this condition.

As evident from Fig. 7, the lowest %-R1 (82.86%) and %-R2 (86.34%) were noted for composite alternative A1 having 2.5 wt% *Grewia optiva* fiber content and both %-R1 (102.80%) and %-R2 (98.30%) remained highest in the alternative A6 with 6 wt% of rice husk ash content. Also, the composite alternative A3 having 7.5 wt% *Grewia optiva* fiber shows the lowest %-R3 (81.20%) and alternative A5 with 6 wt% rice husk shows the highest %-R3 (103.08%). Regarding the recovery performance (%-R1, %-R2 and %-R3 - the higher, the better), considering a simplified analysis (pass or fail) and assuming recovery performance $\geq$90 for a pass criterion, it is seen that all *Grewia optiva* samples have failed, since they all presented at least one stage in the recoveries (%-R1, %-R2 and %-R3) where they showed recovery
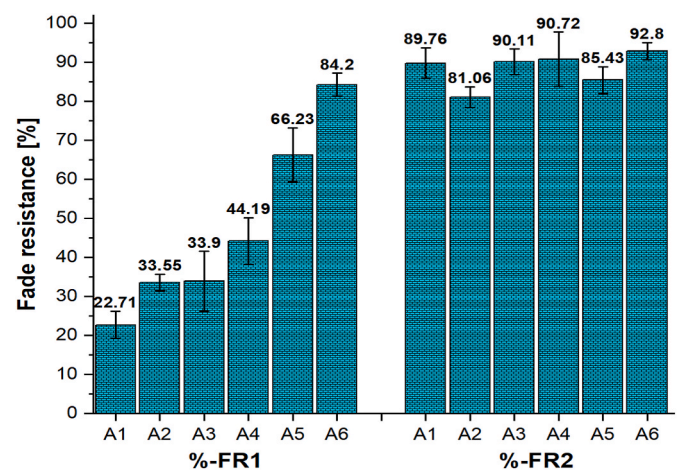
Fig. 5. μ_{avg} and $\Delta\mu$ results of the evaluated composites.

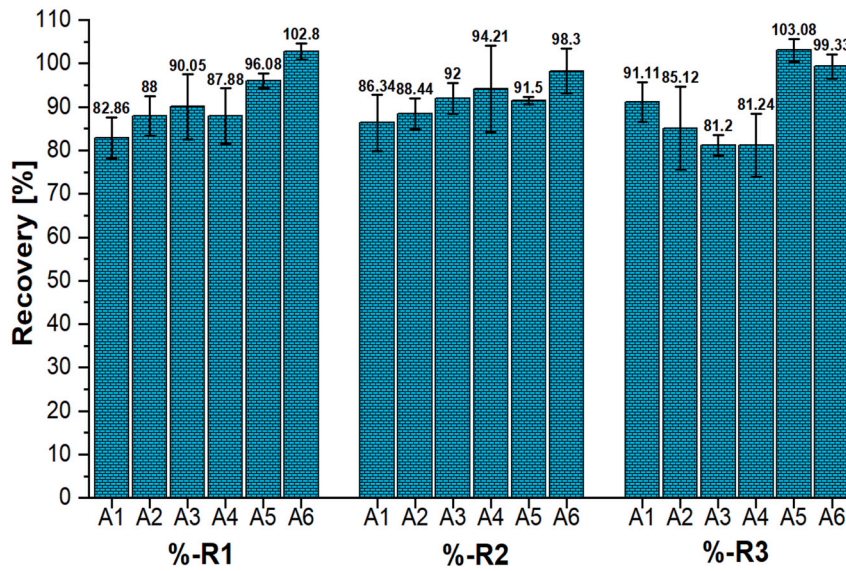**Fig. 6.** %-FR1 and %-FR2 results of the evaluated composites.

Fig. 7. %-R1, %-R2 and %-R3 results of the evaluated composites.

performance <90.

On the other hand, the samples with rice husk and rice husk ash exhibited good performance throughout the recovery sections. As the recoveries are placed immediately after high temperature sections (fade 1, TPS and fade 2), a poor performance in those sections is also expected to be reflected in the recoveries. As *Grewia optiva* samples exhibited greater losses in friction compared to husk and rice husk ash during the high temperature sections, the respective recoveries in friction also last longer, which makes the %-R1, %-R2 and %-R3 perform poorly. On the other hand, A5 and A6 passed in the criterion for recovery performance ≥90, meaning that those formulations have a good balance between fibers (rice husk and rice husk ash) and the basic materials.

3.2. SEM images of the material's surfaces

As discussed previously, the superior fade resistance presented by the friction material with rice husk ash was linked to the greater content of contact plateaus formed on the surface of the material, as can be seen on
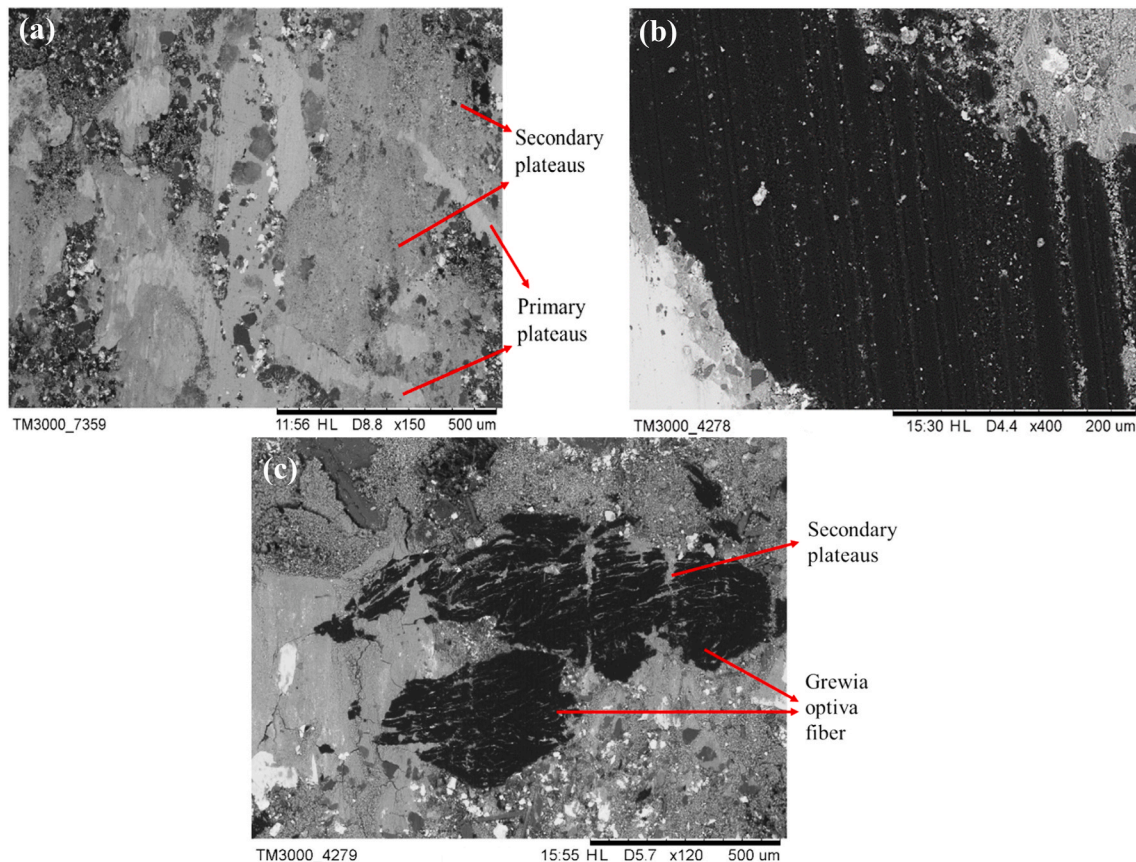

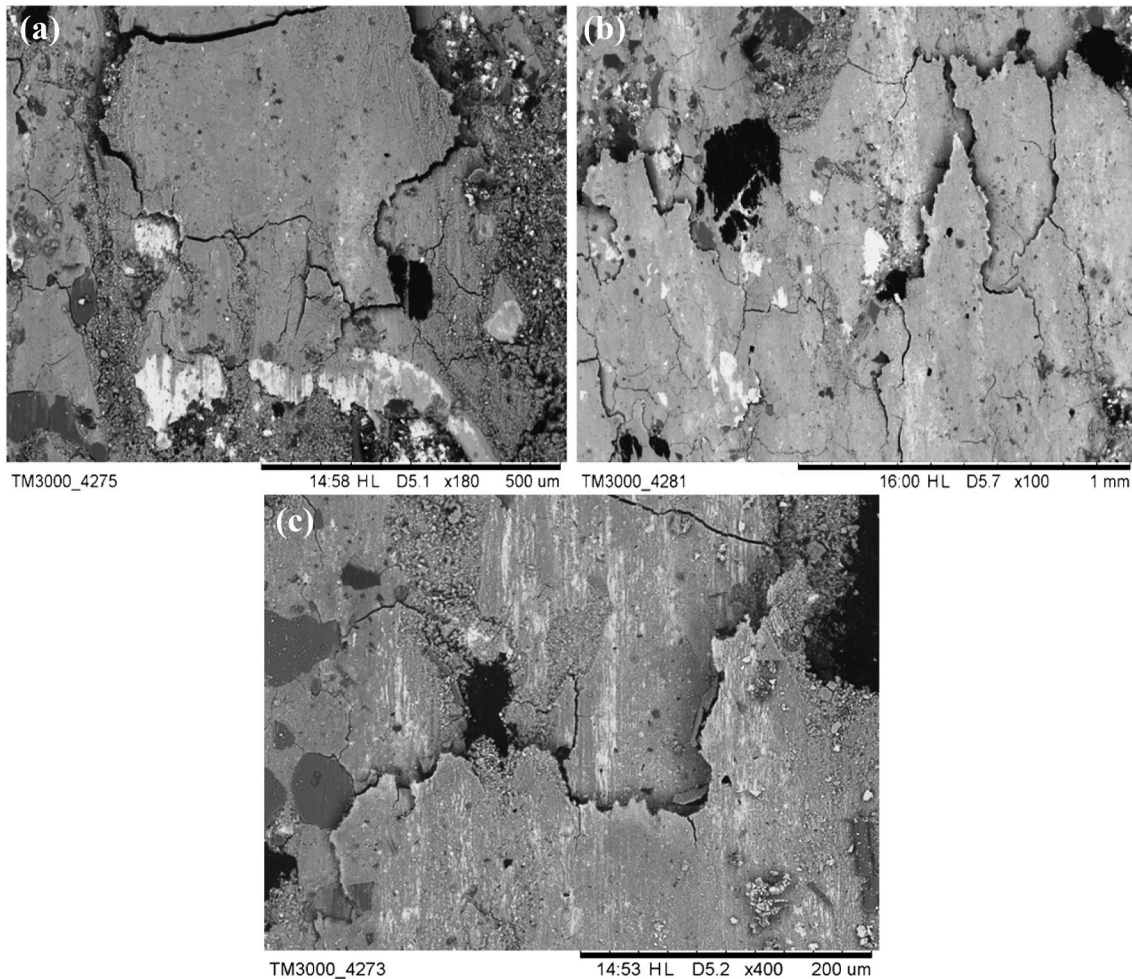**Fig. 8.** SEM images of the worn surface of composites (a) A6, (b) A2, and (c) A3.

Fig. 8a. The rice husk ash particle assists in the formation of contact plateaus. One of the main wear mechanisms observed in all samples is abrasion, as exemplified by the grooves seen on the *Grewia optiva* fiber in Fig. 8b.

Previous studies [31,34,39] have shown that the presence of porous fibers promotes the development of secondary plateaus without the support of primary plateaus. Those contact plateaus are known as type 2 [59], to distinguish them from the contact plateaus formed with the support of primary plateaus (type 1) [60,61]. The contact plateaus of type 2 are formed on the top of the porous fibers (*Grewia optiva* or rice husk, as in the present study). This is explained by the capacity the porous fibers have for capturing and storing microscopic particles, acting as a sort of reservoir for those particles, which are then compressed by pressure and sliding. This effect is evidenced by Fig. 8c; where part of the surface of a *Grewia optiva* fiber is covered by secondary plateaus.

Besides abrasion, another important wear mechanism identified in all samples was the destruction of secondary plateaus through the formation and propagation of cracks, as exemplified in Fig. 9a and b. As explained in Ref. [62], there exists a crucial threshold of tensile strength that causes the secondary contact plateaus to break down. This means that the high pressure exerted during the braking process surpassed the maximum tensile strength of the contact plateaus, resulting in the formation of fractures. Following the development of cracks, the secondary plateaus have a decrease in strength, resulting in the removal of some sections, as seen in Fig. 9c. Delamination of the secondary plateaus occurs because of the sliding contact on the sample's surface. This process (cracks + delamination) was seen for all friction materials (*Grewia optiva*, rice husk and rice husk ash) selected in the present study.

Furthermore, Fig. 10 exhibits the ranks of the composite samples according to their efficacy for each assessed attribute. Fig. 10 unambiguously demonstrates that no one composite sample has surpassed the others in terms of all assessed attributes concurrently. For example, composite sample A2 performed very well in terms of μ_p (0.44) and μ_{avg} (0.510). Nevertheless, it performed poorly regarding SWR (4.00×10^{-7} cm^3/Nm), and %-FR2 (81.06%). Composite A3 has the lowest SWR (3.26×10^{-7} cm^3/Nm), and $\Delta\mu$ (0.197) but stand poorest from %-R3 with a value of 81.20%. Composite A5 has the highest %-R3 (103.08%), second-highest %-R2 (96.08%), second-highest %-FR1 (66.23%), and second-best SWR (3.30×10^{-7} cm^3/Nm) but also exhibits lowest μ_p (0.35), lowest μ_{avg} (0.39), and highest $\Delta\mu$ (0.337). Composite sample A6 had the best %-FR1 (84.20%), %-FR2 (92.80%), %-R1 (102.8%), and %-R2 (98.10%), but it ranked second-last in μ_{avg} (0.448), and $\Delta\mu$ (0.328). Consequently, a comprehensive CRITIC-MARCOS-based MCDM approach was used to rank these samples and identify the most suitable option that satisfies all of these conflicting qualities predominantly. The selection criteria consisted of the examined properties, namely μ_p (C1), SWR (C2), μ_{avg} (C3), $\Delta\mu$ (C4), %-FR1 (C5), %-FR2 (C6), %-FR1 (C7), %-FR2 (C8) and %-FR3 (C9) were taken as selection criteria. The properties C1, C3, C5, C6, C7, C8, and C9 were regarded as advantageous characteristics for automotive brake friction composites, meaning that greater values of these features are preferred (i.e., higher-is-better).

Fig. 9. SEM images of cracked secondary plateaus on surface of composites (a) A1, (b) A3 and (c) delamination of secondary plateaus on the surface of formulation A1.
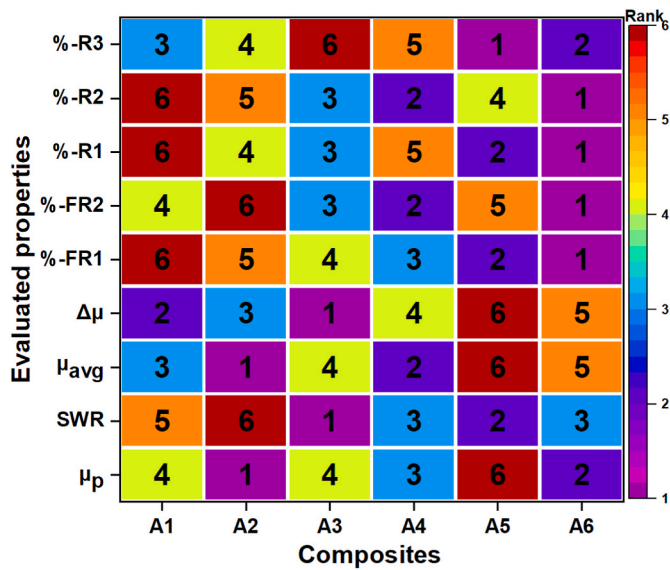
Fig. 10. Ranking of composites for individual criteria.

Simultaneously, criterion C2 and C4 were deemed non-beneficial, meaning that a lower value is preferable (i.e., the lower-is-better).

3.3. Ranking of the composites

3.3.1. Weight calculation

The automotive brake friction composite selection problem consists of nine criteria and six alternatives, which are arranged in the form of a decision matrix in Table 3 using Eq. (1). The procedures described in section 2.3 are followed in order to use the CRITIC technique to calculate the criteria weights. First, r_{ij} values are used to generate the normalized decision matrix in line with Eq. (2) and Eq. (3). The normalized outcomes are shown in Table 4. The second-last row of Table 4 refers to the standard deviation (S_j) of each criterion determined using Eq. (4). Last row of Table 4 shows the values for degree of conflict ($\Re_j$) between criterion determined by using Eq. (5). Afterward, using Eq. (6), the criterion weights are computed as follows: $C1 = 0.1146$, $C2 = 0.1022$, $C3 = 0.1485$, $C4 = 0.1504$, $C5 = 0.0949$, $C6 = 0.0869$, $C7 = 0.0870$, $C8 = 0.0782$, and $C9 = 0.1373$.

3.3.2. Evaluation of alternatives

The decision matrix is formulated following the determination of the ideal value (IV) and anti-ideal value (AIV) via Eq. (8) and Eq. (9), respectively. The structured decision matrix utilized in the MARCOS analysis for the provided alternatives and criteria is displayed in Table 5. Based on the MARCOS procedure mentioned in Section 2.3, each value is normalized by Eq. (10) and Eq. (11). The resulting normalized decision matrix for the MARCOS analysis is demonstrated in Table 6. The weights shown in Table 4 that were calculated using the CRITIC approach are then used to create the weighted decision matrix using Eq. (12). The weighted decision matrix is presented in Table 7. Next, Eq. (13)–(15) of the procedure of MARCOS method are used to obtain the utility degree

(k_i^+, k_i^-) and utility functions ($f(k_i^+), f(k_i^-)$) of alternatives. After that the final utility function ($f(k_i)$) of each alternative is determined using Eq. (16). The results of MARCOS analysis are summarized in Table 8. Finally, the rank is given to alternatives according to the obtained $f(k_i)$ values. As shown in Table 8, the brake friction composite alternatives can be arranged in descending order as A6–A3–A5–A4–A1–A2. It is concluded that the composite A6 which has 6 wt% rice husk ash is selected as the best choice for automotive braking application under the given conditions by considering the nine criteria discussed in section 3.1.

3.4. Comparison with alternative decision-making methods

The primary objective of this part is to provide the CRITIC-MARCOS technique, a contemporary approach in the literature, used for composite ranking. Additionally, it aims to compare this method with eight other well-established ranking systems, offering a valuable chance for comparison. In order to do this, comparisons are made using ARAS [42], MOORA [45], MEW [53], SAW [63], WASPAS [63], COPRAS [64], PSI [65], and MAUT [66]. The chosen methodologies use the same weights obtained from the CRITIC methodology, as employed in the MARCOS ranking, to ensure a fair and equitable comparison. The rankings of alternate composites generated via different procedures are shown in Fig. 11. Alternative A6 is consistently rated as the top choice, whereas alternative A3 is consistently ranked as the second choice in all decision-making procedures used. Fig. 11 revealed that ranking similar to MARCOS is obtained for PSI, MEW, ARAS, WASPAS, COPRAS and MOORA. Whereas alternatives A4/A5 and A1/A2 noted to exchanges the ranking order for MAUT approach. In addition, the statistical test known as Spearman's rank correlation test is used to determine the relationship between the rankings acquired by CRITIC-MARCOS and other decision-making procedures. The rank correlation (RC) between two datasets is computed using Eq. (20) [37,42].

$$\text{RC} = \frac{(p^3 - p) - 6\sum_{i=1}^{p}\delta_i^2}{p^3 - p}, \quad -1 \leq RC \leq +1 \tag{20}$$

Where, p represents alternatives and δ_i is the difference in the ranks of two datasets.

A correlation coefficient of 1 was achieved between the rank of the MARCOS technique and the PSI, MEW, ARAS, WASPAS, COPRAS, and MOORA methods, whereas it was 0.89 for MAUT. The high correlation between rankings demonstrates the stability and resilience of the combined CRITIC-MARCOS approach. The suggested approach may be used for insightful and rational decision-making in the evaluation and selection of automobile brake friction composite material.

4. Conclusions

The selection of automotive brake friction material is a complex topic that significantly affects the tribological performance. To identify the best brake friction formulation with optimal tribological properties, an integrated CRITIC-MARCOS technique was devised. Six compositions, including rice husk, rice husk ash, and Grewia optiva fiber, were produced and assessed for their tribological properties using a laboratory-scale brake tribometer, following the SAE J2522 test procedure. The

Table 3
Decision matrix for CRITIC analysis.

Alternatives	C1	C2	C3	C4	C5	C6	C7	C8	C9
A1	0.41	3.70×10^{-7}	0.494	0.243	22.71	89.76	82.86	86.34	91.11
A2	0.44	4.00×10^{-7}	0.510	0.291	33.55	81.06	88.00	88.44	85.12
A3	0.41	3.26×10^{-7}	0.482	0.197	33.90	90.11	90.05	92.00	81.20
A4	0.42	3.40×10^{-7}	0.506	0.324	44.19	90.72	87.88	94.21	81.24
A5	0.35	3.30×10^{-7}	0.390	0.337	66.23	85.43	96.08	91.50	103.08
A6	0.43	3.40×10^{-7}	0.448	0.328	84.20	92.80	102.8	98.30	99.33

Table 4
Decision matrix normalization for CRITIC analysis.

Alternatives	C1	C2	C3	C4	C5	C6	C7	C8	C9
A1	0.6667	0.4054	0.8667	0.6714	0.0000	0.7411	0.0000	0.0000	0.4529
A2	1.0000	0.0000	1.0000	0.3286	0.1763	0.0000	0.2578	0.1756	0.1792
A3	0.6667	1.0000	0.7667	1.0000	0.1820	0.7709	0.3606	0.4732	0.0000
A4	0.7778	0.8108	0.9667	0.0929	0.3493	0.8228	0.2518	0.6580	0.0018
A5	0.0000	0.9459	0.0000	0.0000	0.7078	0.3722	0.6630	0.4314	1.0000
A6	0.8889	0.8108	0.4833	0.0643	1.0000	1.0000	1.0000	1.0000	0.8286
S_j	0.3514	0.3855	0.3816	0.3990	0.3781	0.3657	0.3550	0.3533	0.4274
$\Re_j$	8.276	6.7282	9.8746	9.5619	6.3698	6.0287	6.2149	5.6152	8.1479
ω_j	0.1146	0.1022	0.1485	0.1504	0.0949	0.0869	0.0870	0.0782	0.1373

Table 5
Extended decision matrix for MARCOS analysis.

Alternatives	C1	C2	C3	C4	C5	C6	C7	C8	C9
AIV	0.35	4.00×10^{-7}	0.390	0.337	22.71	81.06	82.86	86.34	81.20
A1	0.41	3.70×10^{-7}	0.494	0.243	22.71	89.76	82.86	86.34	91.11
A2	0.44	4.00×10^{-7}	0.510	0.291	33.55	81.06	88.00	88.44	85.12
A3	0.41	3.26×10^{-7}	0.482	0.197	33.90	90.11	90.05	92.00	81.20
A4	0.42	3.40×10^{-7}	0.506	0.324	44.19	90.72	87.88	94.21	81.24
A5	0.35	3.30×10^{-7}	0.390	0.337	66.23	85.43	96.08	91.50	103.08
A6	0.43	3.40×10^{-7}	0.448	0.328	84.20	92.80	102.8	98.30	99.33
IV	0.44	3.26×10^{-7}	0.510	0.197	84.20	92.80	102.80	98.30	103.08

Table 6
Normalized decision matrix for MARCOS analysis.

Alternatives	C1	C2	C3	C4	C5	C6	C7	C8	C9
AIV	0.7955	0.8150	0.7647	0.5846	0.2697	0.8735	0.8060	0.8783	0.7877
A1	0.9318	0.8811	0.9686	0.8107	0.2697	0.9672	0.8060	0.8783	0.8839
A2	1.0000	0.8150	1.0000	0.6770	0.3985	0.8735	0.8560	0.8997	0.8258
A3	0.9318	1.0000	0.9451	1.0000	0.4026	0.9710	0.8760	0.9359	0.7877
A4	0.9545	0.9588	0.9922	0.6080	0.5248	0.9776	0.8549	0.9584	0.7881
A5	0.7955	0.9879	0.7647	0.5846	0.7866	0.9206	0.9346	0.9308	1.0000
A6	0.9773	0.9588	0.8784	0.6006	1.0000	1.0000	1.0000	1.0000	0.9636
IV	1.0000	1.0000	1.0000	1.0000	1.0000	1.0000	1.0000	1.0000	1.0000

Table 7
Weighted normalized decision matrix for MARCOS analysis.

Alternatives	C1	C2	C3	C4	C5	C6	C7	C8	C9
AIV	0.0912	0.0833	0.1136	0.0879	0.0256	0.0759	0.0701	0.0687	0.1082
A1	0.1068	0.0900	0.1438	0.1219	0.0256	0.0841	0.0701	0.0687	0.1214
A2	0.1146	0.0833	0.1485	0.1018	0.0378	0.0759	0.0745	0.0704	0.1134
A3	0.1068	0.1022	0.1403	0.1504	0.0382	0.0844	0.0762	0.0732	0.1082
A4	0.1094	0.0980	0.1473	0.0914	0.0498	0.0850	0.0744	0.0749	0.1082
A5	0.0912	0.1010	0.1136	0.0879	0.0746	0.0800	0.0813	0.0728	0.1373
A6	0.1120	0.0980	0.1304	0.0903	0.0949	0.0869	0.0870	0.0782	0.1323
IV	0.1146	0.1022	0.1485	0.1504	0.0949	0.0869	0.0870	0.0782	0.1373

Table 8
MARCOS results.

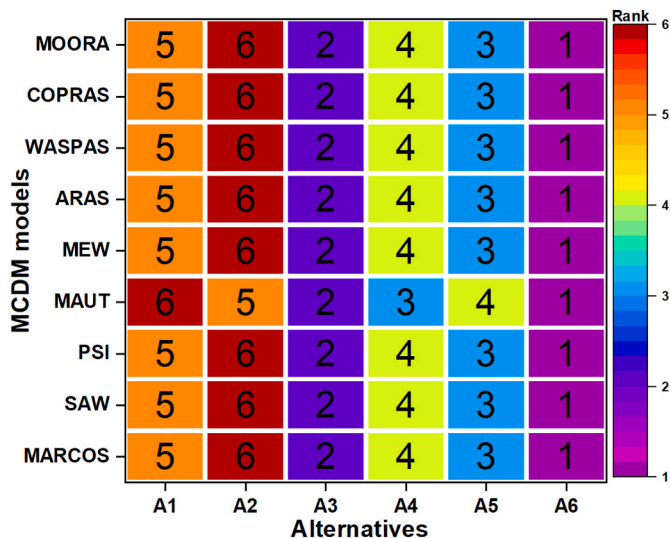| Alternatives	k_i	k_i^-	k_i^+	$f(k_i^-)$	$f(k_i^+)$	$f(k_i)$	Rank
AIV	0.7244						
A1	0.8324	1.1491	0.8324	0.4201	0.5799	0.6382	5
A2	0.8201	1.1322	0.8201	0.4201	0.5799	0.6288	6
A3	0.8799	1.2146	0.8799	0.4201	0.5799	0.6746	2
A4	0.8385	1.1574	0.8385	0.4201	0.5799	0.6428	4
A5	0.8396	1.1591	0.8396	0.4201	0.5799	0.6437	3
A6	0.9101	1.2563	0.9101	0.4201	0.5799	0.6977	1
IV	1.0000						

Fig. 11. Ranking of composites using various decision-making approaches.

tribological findings, which included the coefficient of friction, frictional fluctuations, specific wear rate, fade, and recovery performances, were used as evaluation criteria for determining the composite ranking. The CRITIC method was used to allocate weights to the chosen criteria, whilst the MARCOS approach was implemented to ascertain the ranking of the composites. The findings of the CRITIC-MARCOS method indicate that the formulation containing 6 wt% rice husk ash has the most favorable tribological properties. In addition, identical rankings were achieved for the provided criteria and alternatives using SAW, PSI, MEW, ARAS, WASPAS, COPRAS, and MOORA methodologies. The Spearman's rank correlation coefficients between the proposed approach and various MCDM methods, ranging from 0.89 to 1, demonstrate the consistency of the rankings across different methodologies and highlighting the stability of the ranking results. The study proposed an integrated CRITIC-MARCOS technique to deal with the issue of material selection when the criterion weights are inherently contradictory. The approach's efficacy and straightforwardness make it suitable for a broader array of materials selection and advance sustainability by using agro-waste and natural fibers to create green products such as automotive brake friction composite materials.

CRediT authorship contribution statement

Tej Singh: Writing – review & editing, Writing – original draft, Visualization, Validation, Resources, Project administration, Methodology, Investigation, Formal analysis, Conceptualization. **Gustavo da Silva Gehlen:** Writing – review & editing, Writing – original draft, Investigation, Formal analysis, Data curation. **Vedant Singh:** Writing – review & editing, Visualization, Methodology, Formal analysis. **Ney Francisco Ferreira:** Writing – review & editing, Visualization, Investigation, Formal analysis. **Liu Yesukai de Barros:** Writing – review & editing, Formal analysis, Data curation. **Germano Lasch:** Writing – review & editing, Formal analysis, Data curation. **Jean Carlos Poletto:** Writing – review & editing, Formal analysis, Data curation. **Sharafat Ali:** Writing – review & editing, Formal analysis, Data curation. **Patric Daniel Neis:** Writing – review & editing, Investigation, Formal analysis, Data curation, Writing – original draft.

Declaration of competing interest

The authors declare that they have no known competing financial interests or personal relationships that could have appeared to influence the work reported in this paper.

Data availability

Data will be made available on request.

References

[1] O.I. Adeyemi, K. Kirwan, I. Tuersley, S.R. Coles, Comparative assessment of the performance of friction materials based on different agricultural wastes, Tribol. Int. 191 (2024) 109130.

[2] Q. Zhang, Z. Qi, Y. Yao, Y. Ma, D. Zhang, M. Chen, D. Ren, Potential reinforcing properties of silane-modified rapeseed straw fibers in friction composites: fractal dimension and circularity characterise powder flowability, Ind. Crop. Prod. 206 (2023) 117644.

[3] UNECE (United Nations Economic Commission for Europe) Regulation 90, Uniform Provisions Concerning the Approval of Replacement Brake Lining Assemblies, Drum Brake Linings and Discs and Drums for Power-Driven Vehicles and Their Trailers, 2012. E/ECE/324/Rev.1/Add.89/Rev.3. February.

[4] Commission Proposes New Euro 7 Standards to Reduce Pollutant Emissions from Vehicles and Improve Air Quality, European Commission, Brussels, 2022, pp. 1–3.

[5] F. Varriale, D. Carlevaris, J. Wahlström, V. Malmborg, Y. Lyu, On the impact of pad material ingredients on particulate wear emissions from disc brakes, Results in Engineering 19 (2023) 101397.

[6] D. Saha, D. Sharma, B.K. Satapathy, Challenges pertaining to particulate matter emission of toxic formulations and prospects on using green ingredients for sustainable eco-friendly automotive brake composites, Sustainable Materials and Technologies 37 (2023) e00680.

[7] K. Yu, X. Shang, X. Zhao, L. Fu, X. Zuo, H. Yang, High frictional stability of braking material reinforced by Basalt fibers, Tribol. Int. 178 (2023) 108048.

[8] Y. Liu, X. Gui, J. Li, S. Zhou, Y. Wang, W. Jia, A. Shi, Q. Yang, M. Ou, Y. Ma, J. Tong, Influence of CSF/GF ratio on tribological behavior of hybrid fiber-reinforced braking friction materials, Tribol. Int. 180 (2023) 108244.

[9] P. Monreal-Perez, D. Elduque, D. López, I. Sola, J. Yaben, I. Clavería, Full-scale dynamometer tests of composite railway brake shoes including latxa sheep wool fibers, J. Clean. Prod. 379 (2022) 134533.

[10] F. Ahmadijokani, A. Shojaei, S. Dordanihaghighi, E. Jafarpour, S. Mohammadi, M. Arjmand, Effects of hybrid carbon-aramid fiber on performance of non-asbestos organic brake friction composites, Wear 452–453 (2020) 203280.

[11] S. Navaratnam, K. Selvaranjan, D. Jayasooriya, P. Rajeev, J. Sanjayan, Applications of natural and synthetic fiber reinforced polymer in infrastructure: a suitability assessment, J. Build. Eng. 66 (2023) 105835.

[12] S.H. Park, Types and health hazards of fibrous materials used as asbestos substitutes, Safety and Health at Work 9 (2018) 360–364.

[13] I. Elfaleh, F. Abbassi, M. Habibi, F. Ahmad, M. Guedri, M. Nasri, C. Garnier, A comprehensive review of natural fibers and their composites: an eco-friendly alternative to conventional materials, Results in Engineering 19 (2023) 101271.

[14] L. Lendvai, Lignocellulosic agro-residue/polylactic acid (PLA) biocomposites: rapeseed straw as a sustainable filler, Cleaner Materials 9 (2023) 100196.

[15] N. de Beus, M. Carus, M. Barth, Carbon Footprint and Sustainability of Different Natural Fibres for Biocomposites and Insulation Material, 2019. http://eiha.org /media/2019/03/19-03-13-Study-Natural-Fibre-Sustainability-Carbon-Footprint. pdf.

[16] M.A. Karim, M.Z. Abdullah, A.F. Deifalla, M. Azab, A. Waqar, An assessment of the processing parameters and application of fibre-reinforced polymers (FRPs) in the petroleum and natural gas industries: a review, Results in Engineering 18 (2023) 101091.

[17] M.M. Rahman, M. Maniruzzaman, M.S. Yeasmin, A state-of-the-art review focusing on the significant techniques for naturally available fibers as reinforcement in sustainable bio-composites: extraction, processing, purification, modification, as well as characterization study, Results in Engineering 20 (2023) 101511.

[18] O. Sanni, J. Ren, T.-C. Jen, Agro-industrial wastes as corrosion inhibitor for 2024-T3 aluminum alloy in hydrochloric acid medium, Results in Engineering 16 (2022) 100676.

[19] G. Akıncıoğlu, H. Öktem, İ. Uygur, S. Akıncıoğlu, Determination of friction-wear performance and properties of eco-friendly brake pads reinforced with hazelnut shell and boron dusts, Arabian J. Sci. Eng. 43 (2018) 727–4737.

[20] G. Akıncıoğlu, S. Akıncıoğlu, H. Öktem, İ. Uygur, Wear response of non-asbestos brake pad composites reinforced with walnut shell dust, Journal of the Australian Ceramic Society 56 (2020) 1061–1072.

[21] J. Chandradass, M.A. Surabhi, P.B. Sethupathi, P. Jawahar, Development of low cost brake pad material using asbestos free sugarcane bagasse ash hybrid composites, in: Materials Today: Proceedings, 2021, pp. 7050–7057, 45.

[22] S. Choosri, N. Sombatsompop, E. Wimolmala, S. Thongsang, Potential use of fly ash and bagasse ash as secondary abrasives in phenolic composites for eco-friendly brake pads applications, in: Proceedings of the Institution of Mechanical Engineers, Part D: Journal of Automobile Engineering, 2019, pp. 1296–1305, 233.

[23] P.W. Olupot, E. Menya, F. Lubwama, L. Ssekaluvu, B. Nabuuma, J. Wakatuntu, Effects of sawdust and adhesive type on the properties of rice husk particleboards, Results in Engineering 16 (2022) 100775.

[24] J. Wakatuntu, P.W. Olupot, J. Jjagwe, E. Menya, M. Okure, Optimization of pyrolysis conditions for production of rice husk-based bio-oil as an energy carrier, Results in Engineering 17 (2023) 100947.

[25] M. Kordi, N. Farrokhi, M.I. Pech-Canul, A. Ahmadikhah, Rice husk at a glance: from agro-industrial to modern applications, Rice Sci. (2023), https://doi.org/ 10.1016/j.rsci.2023.08.005.

[26] R. Khargotra, T. Alam, K. Thu, V. Sebestyén, K. András, T. Singh, Experimental study of eco-friendly insulating materials for solar thermal collectors: a sustainable built environment, Results in Engineering (2023) 101681.

[27] K. Homchat, S. Ramphueiphad, The continuous carbonisation of rice husk on the gasifier for high yield charcoal production, Results in Engineering 15 (2022) 100495.

[28] M.A. Khan, S.A. Khan, B. Khan, K. Shahzada, F. Althoey, A.F. Deifalla, Investigating the feasibility of producing sustainable and compatible binder using marble waste, fly ash, and rice husk ash: a comprehensive research for material characteristics and production, Results in Engineering 20 (2023) 101435.

[29] I. Mutlu, Investigation of tribological properties of brake pads by using rice straw and rice husk dust, J. Appl. Sci. 9 (2009) 377–381.

[30] I. Mutlu, A. Keskin, Wear behavior of rice straw powder in automotive brake pads, Mater. Test. 63 (2021) 458–461.

[31] G.S. Gehlen, P.D. Neis, L.Y. Barros, J.C. Poletto, N.F. Ferreira, S.C. Amico, Tribological performance of eco-friendly friction materials with rice husk, Wear 500–501 (2022) 204374.

[32] A.P.G. Nogueira, G.S. Gehlen, P.D. Neis, N.F. Ferreira, S. Gialanella, G. Straffelini, Rice husk as a natural ingredient for brake friction material: a pin-on-disc investigation, Wear 494–495 (2022) 204272.

[33] D. Carlevaris, M. Leonardi, G. Straffelini, S. Gialanella, Design of a friction material for brake pads based on rice husk and its derivatives, Wear 526–527 (2023) 204803.

[34] G.S. Gehlen, A.P.G. Nogueira, D. Carlevaris, L.Y. Barros, J.C. Poletto, G. Lasch, G. Straffelini, N.F. Ferreira, P.D. Neis, Tribological assessment of rice husk ash in eco-friendly brake friction materials, Wear 516–517 (2023) 204613.

[35] M.J. Ahmed, M.A.S. Balaji, S.S. Saravanakumar, P. Senthamaraikannan, Characterization of *Areva javanica* fiber-A possible replacement for synthetic acrylic fiber in the disc brake pad, J. Ind. Textil. 49 (2019) 294–317.

[36] A. Mustafa, M.F.B. Abdollah, F.F. Shuhimi, N. Ismail, H. Amiruddin, N. Umehara, Selection and verification of kenaf fibres as an alternative friction material using weighted decision matrix method, Mater. Des. 67 (2015) 577–582.

[37] T. Singh, V. Singh, L. Ranakoti, S. Kumar, Optimization on tribological properties of natural fiber reinforced brake friction composite materials: effect of objective and subjective weighting methods, Polym. Test. 117 (2023) 107873.

[38] R. Rajan, Y.K. Tyagi, S. Singh, Waste and natural fiber based automotive brake composite materials: influence of slag and coir on tribological performance, Polym. Compos. 43 (2022) 1508–1517.

[39] T. Singh, G.S. Gehlen, N.F. Ferreira, L.Y. Barros, G. Lasch, J.C. Poletto, S. Ali, P. D. Neis, Automotive brake friction composite materials using natural *Grewia Optiva* fibers, J. Mater. Res. Technol. 26 (2023) 6966–6983.

[40] T. Singh, A hybrid multiple-criteria decision-making approach for selecting optimal automotive brake friction composite, Material Design & Processing Communications 3 (2021) e266.

[41] R. Kumar, S. Kumar, Ü. Ağbulut, A.E. Gürel, M. Alwetaishi, S. Shaik, C.A. Saleel, D. Lee, Parametric optimization of an impingement jet solar air heater for active green heating in buildings using hybrid CRITIC-COPRAS approach, Int. J. Therm. Sci. 197 (2024) 108760.

[42] V.D. Baloyi, L.D. Meyer, The development of a mining method selection model through a detailed assessment of multi-criteria decision methods, Results in Engineering 8 (2020) 100172.

[43] Z. Gao, R.Y. Liang, T. Xuan, VIKOR method for ranking concrete bridge repair projects with target-based criteria, Results in Engineering 3 (2019) 100018.

[44] P.P. Dwivedi, D.K. Sharma, Application of Shannon Entropy and COCOSO techniques to analyze performance of sustainable development goals: the case of the Indian Union Territories, Results in Engineering 14 (2022) 100416.

[45] H.H. Başaran, İ. Tarhan, Investigation of offshore wind characteristics for the northwest of Türkiye region by using multi-criteria decision-making method (MOORA), Results in Engineering 16 (2022) 100757.

[46] T. Singh, Utilization of cement bypass dust in the development of sustainable automotive brake friction composite materials, Arab. J. Chem. 14 (2021) 103324.

[47] O.M. Olabanji, K. Mpofu, Appraisal of conceptual designs: coalescing fuzzy analytic hierarchy process (F-AHP) and fuzzy grey relational analysis (F-GRA), Results in Engineering 9 (2021) 100194.

[48] Ž. Stević, D. Pamučar, A. Puška, P. Chatterjee, Sustainable supplier selection in healthcare industries using a new MCDM method: measurement of alternatives and ranking according to compromise solution (MARCOS), Comput. Ind. Eng. 140 (2020) 106231.

[49] D. Diakoulaki, G. Mavrotas, L. Papayannakis, Determining objective weights in multiple criteria problems: the critic method, Comput. Oper. Res. 22 (1995) 763–770.

[50] P.D. Neis, N.F. Ferreira, F.J. Lorini, Contribution to perform high temperature tests (fading) on a laboratory-scale tribometer, Wear 271 (2011) 2660–2664.

[51] R.P. Pavlak, P.D. Neis, J.C. Poletto, L.Y. de Barros, N.F. Ferreira, Wear, Friction and NVH Characterization Using a Laboratory-Scale Tribometer (No. 2017-36-0003), 2017. SAE Technical Paper.

[52] A.M. Martinez, J. Echeberria, Towards a better understanding of the reaction between metal powders and the solid lubricant Sb_2S_3 in a low-metallic brake pad at high temperature, Wear 348–349 (2016) 27–42.

[53] T. Singh, Optimum design based on fabricated natural fiber reinforced automotive brake friction composites using hybrid CRITIC-MEW approach, J. Mater. Res. Technol. 14 (2021) 81–92.

[54] A.E. Torkayesh, S.E. Torkayesh, Evaluation of information and communication technology development in G7 countries: an integrated MCDM approach, Technol. Soc. 66 (2021) 101670.

[55] S.S.H. Dehshiri, B. Firoozabadi, A new application of measurement of alternatives and ranking according to compromise solution (MARCOS) in solar site location for electricity and hydrogen production: a case study in the southern climate of Iran, Energy 261 (2022) 125376.

[56] A. Abdulla, G. Baryannis, I. Badi, An integrated machine learning and MARCOS method for supplier evaluation and selection, Decision Analytics Journal 9 (2023) 100342.

[57] A. Patnaik, M. Kumar, B.K. Satapathy, B.S. Tomar, Performance sensitivity of hybrid phenolic composites in friction braking: effect of ceramic and aramid fibre combination, Wear 269 (2010) 891–899.

[58] A. Cristol-Bulthé, Y. Desplanques, G. Degallaix, Y. Berthier, Mechanical and chemical investigation of the temperature influence on the tribological mechanisms occurring in OMC/Cast iron friction contact, Wear 264 (2007) 815–825.

[59] P.D. Neis, N.F. Ferreira, G. Fekete, L.T. Matozo, D. Masotti, Towards a better understanding of the structures existing on the surface of brake pads, Tribol. Int. 105 (2017) 135–147.

[60] T. Singh, Tribological performance of volcanic rock (perlite) filled phenolic based brake friction composites, Journal of King Saud University - Engineering Sciences (2021), https://doi.org/10.1016/j.jksues.2021.12.010.

[61] T. Singh, Comparative performance of barium sulphate and cement by-pass dust on tribological properties of automotive brake friction composites, Alex. Eng. J. 72 (2023) 339–349.

[62] L.Y. Barros, J.C. Poletto, G.S. Gehlen, G. Lasch, P.D. Neis, A. Ramalho, N. F. Ferreira, Transition in wear regime during braking applications: an analysis of the debris and surfaces of the brake pad and disc, Tribol. Int. 189 (2023) 108968.

[63] A.K. Yadav, K. Singh, N.I. Arshad, A. Ferrara, A. Ahmadian, Y.I. Mesalam, MADM-based network selection and handover management in heterogeneous network: a comprehensive comparative analysis, Results in Engineering 21 (2024) 101918.

[64] A. Baroutaji, A. Arjunan, G. Singh, J. Robinson, Crushing and energy absorption properties of additively manufactured concave thin-walled tubes, Results in Engineering 14 (2022) 100424.

[65] V.K. Pathak, R. Singh, S. Gangwar, Optimization of three-dimensional scanning process conditions using preference selection index and metaheuristic method, Measurement 146 (2019) 653–667.

[66] C. Çetinkaya, M. Erbaş, M. Kabak, E. Özceylan, A mass vaccination site selection problem: an application of GIS and entropy-based MAUT approach, Soc. Econ. Plann. Sci. 85 (2023) 101376.